Journal of Applied Polymer Science

Microstructure relaxation process of polyhexafluoropropylene after swelling in supercritical carbon dioxide

N. A. Belov,[1] A. Yu. Alentiev,[1] I. A. Ronova,[2] O. V. Sinitsyna,[2] A. Yu. Nikolaev,[2] A. A. Zharov[3]

[1]Topchiev Institute of Petrochemical Synthesis, Leninskii Prospect 29, Moscow 119991, Russia

[2]Nesmeyanov Institute of Organoelement Compounds, Vavilov Street 28, Moscow 119991, Russia

[3]Zelinsky Institute of Organic Chemistry of Russian Academy of Sciences, Leninsky Prospect 47, Moscow 119991, Russia

Correspondence to: I. A. Ronova (E-mail: ron@ineos.ac.ru)

ABSTRACT: This paper studies the process of relaxation of a polymer after swelling in supercritical carbon dioxide. Polyhexafluoropropylene (PHFP) was chosen as the object for investigation. The relaxation process was monitored by a change of the permeability coefficients for a number of gases. Thin polymeric films of PHFP were modified by different treatments: drying to a constant weight, annealing at a temperature slightly higher than the glass-transition temperature, and swelling in supercritical carbon dioxide. The permeability coefficients of six gases, He, H_2, O_2 N_2, CO_2, and CH_4, were measured after each stage of the treatment. It was shown that the permeability coefficients in the films were increased by 2.4 times for He, 3.6 for H_2, 5.9 for O_2, 8.1 for N_2, 6.7 for CO_2, and 10.9 for methane. The permeability coefficients of the same gases were measured 50 days later after swelling in supercritical carbon dioxide. A decrease in the permeability coefficient demonstrated that the relaxation process had taken place. Nevertheless, the values exceeded the initial ones for annealed samples by 2.0 times for He, 2.4 for H_2, 1.8 for O_2, 1.7 for N_2, 1.7 for CO_2, and 1.3 for methane. © 2015 Wiley Periodicals, Inc. J. Appl. Polym. Sci. **2016**, *133*, 43105.

KEYWORDS: in sc-CO_2; membranes; microstructure; packaging; permeability coefficient; swelling; thin film

Received 8 December 2014; accepted 25 October 2015

DOI: 10.1002/app.43105

INTRODUCTION

The greatest progress in membrane science over the last few decades has been achieved in the field of the relationship between the chemical structure of polymer materials and their gas permeation parameters.[1,2] Variations of the design of the elementary unit affect chain stiffness, the packing density of macromolecules, the free volume as found for example by the simplest Bondi method or measured using sophisticated physical techniques such as positron annihilation lifetime spectroscopy,[3] and, hence, their gas permeability and diffusion coefficients. The Robeson diagram of permselectivity versus permeability is a well-accepted method for demonstrating the gas-separation characteristics of polymers with varying structures of elementary units.[4,5] But there is a lot of evidence that not only the chemical structure, but also physical aging,[6–8] the scale effect,[9,10] interactions with a residual solvent,[11] and some methods of posttreatment (for instance, see ref. 12) can affect significantly the permeability and selectivity of polymers. The exposure of various polymers to supercritical CO_2 has been the subject of fundamental and practical efforts. It was shown by positron annihilation lifetime spectroscopy[13–15] and by pressure–volume–temperature measurements[14] that the fraction of free volume in polymers can be increased during the exposure to sc-CO_2. The posttreatment in sc-CO_2 has been also demonstrated to result in highly porous (up to 70 vol %) polymeric materials.[16] Hence, such a level of porosity is successive for gas-separation polymers and must lead to gas defected layers where the Knudsen selectivity of gases is realized.[17]

Recently, an increase of the free volume by 20% and a corresponding increase in gas permeability coefficient has been achieved by swelling of several poly(ether imide) materials in sc-CO_2.[18] The permeability coefficients of these rigid polymers showed no change over a year. In this work, this technique is applied to a new perfluorinated polymer, polyhexafluoropropylene (PHFP),[19] to improve gas permeation parameters. Particular attention will be given to the aging behavior of polymeric films treated in sc-CO_2.

CALCULATION METHODS

In order to correlate the geometry of the repeating units of polymers with transport properties, the following parameters

Additional Supporting Information may be found in the online version of this article.

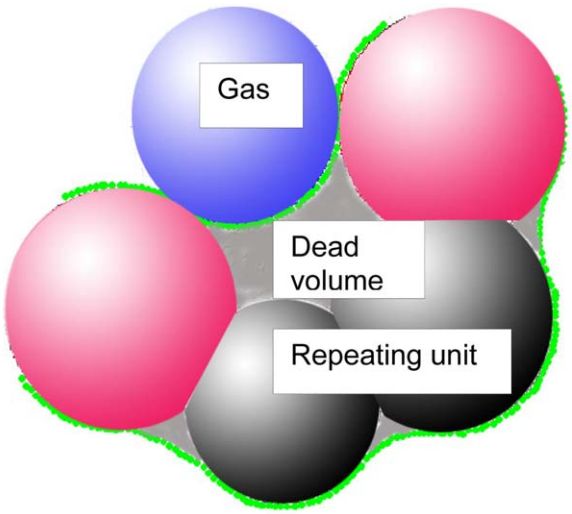

Figure 1. The definitions of free and dead volumes. [Color figure can be viewed in the online issue, which is available at wileyonlinelibrary.com.]

were calculated: van der Waals volume (V_w), free volume (V_f), occupied volume (V_{occ}), accessible volume (V_{acc}), and fractional accessible volume (FAV).[20,21]

For the calculation of accessible volume (V_{acc}), we consider the occupied volume (V_{occ}) and van der Vaals volume (V_w). The occupied volume (V_{occ}) of a repeating unit is given by eq. (1) as being the sum of the Van der Waals volume (V_w) of the repeating unit and the volume of space around this unit that is not accessible for a given type of gas molecule, which is named "dead volume" (V_{dead}) (Figure 1). It is evident that the occupied volume of a repeating unit depends on the size of the gas molecule:

$$V_{occ} = V_w + V_{dead} \quad (1)$$

The accessible volume of a polymer (V_{acc}) is given by eq. (2), where $N_A = 6.02 \times 10^{23}$ is Avogadro's number, ρ is the polymer density, and M_o is the molecular weight of the repeating unit:

$$V_{acc} = \frac{1}{\rho} - \frac{N_A \times V_{occ}}{M_o} \quad (2)$$

However, more often the so-called fractional accessible volume (FAV) is used without any dimensions, which gives a better accordance with the coefficients of diffusion and of permeability, and it is given by eq. (3)[22,23]:

$$FAV = V_{acc} \times \rho \quad (3)$$

To calculate the Van der Waals and the occupied volume of the repeating unit, we used the method described in ref. 21. The model monomer unit constructed in a molecular editor was refined by the quantum chemical method AM1.[24] Then the model of the repeating unit is a set of intersecting spheres with center coordinates coinciding with the atom coordinates, and the radii are equal to the Van der Waals radii of the corresponding atoms, as shown in Figure 2.

The Van der Waals volume (V_w) of the repeating unit is the volume of the body of these overlapping spheres. The Van der Waals radii were taken from Ref. 25. The model of the repeating unit was placed in a box with the parameters equal to the maximum size of the repeating unit. The number of random points m that fall into a repeating unit and the total number of tests M were designated by the Monte Carlo method. Their ratio is multiplied by the volume of the box, as seen in eq. (4):

$$V_w = (m/M) V_{box} \quad (4)$$

Then we calculate the dead volume. Since the O_2, N_2, and CO_2 molecules have an ellipsoidal shape, we calculated the dead volume of the two spheres with radii corresponding to the major and minor ellipsoid axes. A total of 10^6 spheres with the radius of the gas was generated for each atom of the repeating unit. The result is a system consisting of a repeating unit surrounded by overlapping spheres of gas. Then, the system is placed in the "box," similar to the one used in the determination of V_w, and random points are generated in the volume of the box.[21] Thus, without making any assumptions about packing of the polymer chains in the glassy state, we can quickly calculate the Van der Waals volume and the occupied and accessible volumes.

The *free volume* (V_f) was calculated with eq. (5):

$$V_f = \frac{1}{\rho} - \frac{N_A \times V_w}{M_o} \quad (5)$$

The value V_f, thus calculated, shows the volume that is not occupied by the macromolecules in 1 cm^3 of polymer film.

EXPERIMENTAL METHODS

Preparation of Polymer Films

The synthesis of the polymer was carried out by thermally induced radical polymerization at rather high pressure (7–10 kbar). The synthesis, kinetics, and mechanism of polymerization of PHFP have been described previously in detail.[26] Gas permeation properties, a free-volume study by PALS, and vapor sorption characterization were also performed.[19] The average viscosity molecular mass of the polymer was as high as 1×10^6 Da.

The products of oligomerization and cyclization and other volatile contaminants formed during the synthesis of the polymer are eliminated by heat treatment of the reaction products at 200°C for two days under a vacuum environment. Thermal gravimetric analysis (TGA) of the treated product (Figure 3, green) showed that no weight change up to 290–300°C

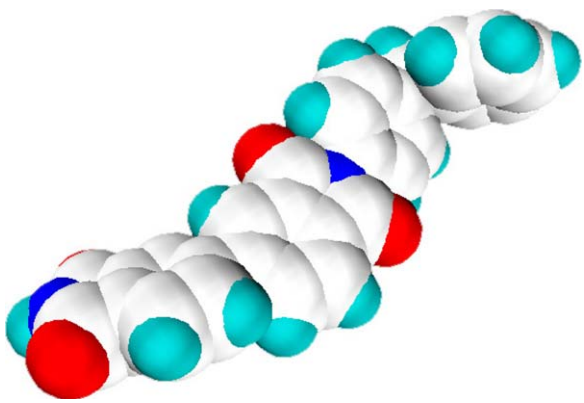

Figure 2. View of the repeating unit with Van der Waals volumes of the atoms. [Color figure can be viewed in the online issue, which is available at wileyonlinelibrary.com.]

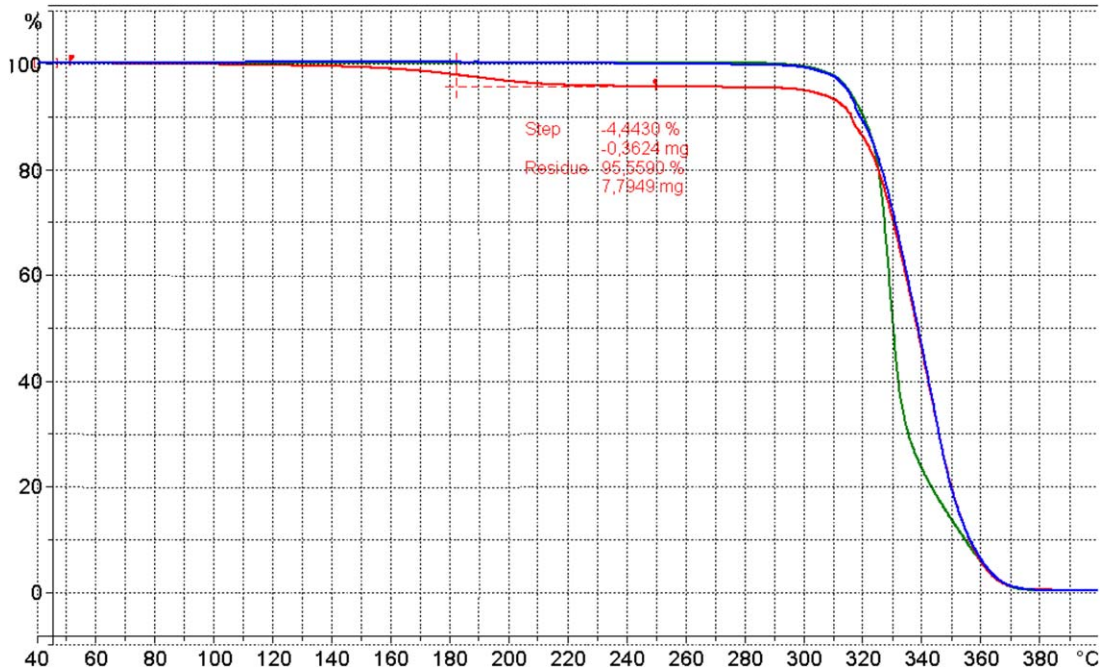

Figure 3. Thermal gravimetric analysis of initial polymer (green), as cast polymeric film with residual solvent (red), and the polymeric film annealed at 160–180°C for 4–5 h (blue) (heat rate is 10 K/min, air flow rate is 80 cm^3/min). [Color figure can be viewed in the online issue, which is available at wileyonlinelibrary.com.]

(a degradation temperature of PHFP) was observed. The polymeric films for subsequent treatments and measurements were cast on a cellophane support from a ~5 wt % solution in octafluorotoluene and dried at room conditions for 4–5 days. Then the polymer films were separated from the cellophane support and evacuated under vacuum to a constant weight. Nevertheless, the films according to TGA and weight loss after annealing at 160–180°C for 4–5 h contained 4.2–4.7 wt % of residual solvent (Figure 3, red). Strictly speaking, the polymer films that have undergone the CO_2 treatment already do not contain the residual solvent (Figure 3, blue). This means that the residual solvent completely leaves the polymer matrix after CO_2 treatment, namely, at swelling in sc-CO_2 and subsequently its desorption.

Therefore, it was decided to produce the final samples swollen in sc-CO_2 starting from two states of the polymeric films: (1) PHFP-fresh, PHFP with ~4.5% of octafluorotoluene, and (2) PHFP-ann, the previous polymeric film annealed at 160–180°C for 4–5 h.

Measurement of Glass-Transition Temperature

The glass-transition temperature (T_g) of the polymers was measured by differential scanning calorimetry (DSC) using a DSC-822e (Mettler-Toledo) apparatus, by using samples of polymer films. The samples were heated at the rate of 10°C/min under nitrogen to above 300°C. Heat flow versus temperature scans from the second heating run were plotted and used for reporting the T_g. The middle point of the inflection curve resulting from the second heating run was assigned as the T_g of the respective polymers. The precision of this method is ±7–10°C.

Measurement of Density

The density of polyimide films was measured using the hydrostatic weighing method that is thoroughly discussed by Yushkin *et al.*[27] The study was performed with equipment for density measurement and an electronic analytic balance Ohaus AP 250D, with precision of 10^{-5} g, from Ohaus Corp. (Parsippany, New Jersey, USA) that was connected to a computer. With this equipment we measured the change of sample weight (density) during the experiment with a precision of 0.001 g/cm^3 in the value of the density. Ethanol and isopropanol were taken as liquids with known density. The studied polyheteroarylenes did not absorb and did not dissolve in these solvents, which for these polymers had low diffusion coefficients. The characteristic diffusion times were in the range of 10^4 to 10^5 s, even for the thinnest films studied here, which leads to longer times, of 1–2 order of magnitude, than that of the density measurement. This is why the sorption of solvent and the swelling of the film must have only an insignificant influence on the value of the measured density. All measurements of the density were performed at 23°C. The density was calculated with eq. (6):

$$\rho_s = \rho_l \times W_a/(W_a - W_l) \quad (6)$$

where ρ_s is density of the sample, W_a is the weight of the sample in air, W_l is the weight of the sample in liquid, and ρ_l is the density of liquid. The error of the density measurements was no higher than 0.3–0.5%.

Method of Treatment with Supercritical Carbon Dioxide (sc-CO_2)

The method of treatment with sc-CO_2 and the experimental apparatus were described in previous papers.[28–31] This experimental apparatus (Figure 4) consists of a pressure generator that can

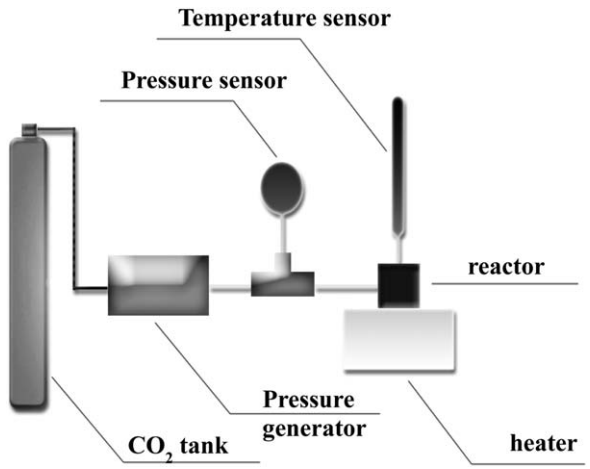

Figure 4. Experimental apparatus for sc-CO_2 treatment.

provide CO_2 pressure up to 35 MPa (High Pressure Equipment Company, Erie, Pennsylvania, USA). A system of valves ensures the CO_2 access to the 30 cm^3 high pressure cell. To control the exposure parameters in the range up to 50 MPa and 120°C, the high-pressure cell was provided with pressure and temperature sensors of 0.1 MPa and 0.2°C accuracy.

To obtain the sc-CO_2 treated films, the following experimental procedure was applied (Figure 5). A polymer film of 20 mm diameter and 30–50 μm thickness was weighed and loaded into the cell (1). The cell was hermetically sealed and purged with CO_2 to remove residual air and water vapor. Temperature and pressure were increased up to experimental values (2), and the film was exposed to reach an equilibrium swelling degree in sc-CO_2 (3). After exposure, the cell was depressurized (4) by regulating the high-pressure valve with an adjustable rate of pressure drop. The treated polymer sample was removed from the cell and transferred (5) onto an analytical balance (AnD GH-252, Tokyo, Japan) to observe and ascertain complete CO_2 desorption (6) from the sample.

Measurement of Transport Parameters

The transport parameters at 25 ± 3°C for He, O_2, N_2, and CO_2 were measured using a mass spectrometric technique[32,33] and barometric techniques on a Balzers QMG 420 quadrupole mass spectrometer (Liechtenstein, Balzers) and an MKS Barotron[19](MKS, Instruments Deutschland GmbH, Germany Munich), respectively. The upstream pressure was 0.8–0.95 atm, and the downstream pressure was about 10^{-3} mm Hg for the spectrometric method, while for the barometric technique tha pressure was in the range of 0.1–1 mm Hg; therefore, the reverse diffusion of penetrating gas was negligible.

The permeability coefficients P were estimated using the formula $P = J_s \times l/\Delta p$, where J_s (cm^3 (STP)/cm^2 s) is the flux of the penetrant gas through 1 cm^2 of the film, Δp (cm Hg) is the pressure drop on the film, and l (cm) is the film thickness.

Morphology of the Films

The surface of the films was investigated by means of the scanning probe microscope FemtoScan (Advanced Technologies Center, Moscow, Russia). Scanning was performed in semi-contact mode at ambient conditions with (MikroMasch, Sofia, Bulgaria) cantilevers of the 15 series. In order to study the bulk microstructure of the films, thin slices are prepared with a thickness as high as 100 nm normal to the surface by means of an ultramicrotome (Ultracut, Reichert-Jung, Vienna, Austria). For the further work, the slices were applied on a copper grid coated by Formvar (polyvinyl formal) film. Then the slices were studied by a transmission electron microscope LEO 912AB OMEGA (Karl Zeiss, Oberkochen, Germany).

RESULTS AND DISCUSSION

The Van der Waals volume, dead volume, and accessible volume for PHFP were calculated. By the above-described procedures, two types of polymeric film samples of PHFP were prepared: dried to a constant weight (sample 1) and annealed to a constant weight at 160–180°C (sample 2). For these samples, densities in propanol-2 and gas permeation by a series of light gases were measured. Then samples were subjected to swelling in sc-CO_2 at 40°C, a pressure of 150 bar, and slow pressure release. After the swelling, the densities of the films and their gas permeation properties were determined again. These densities were used to calculate accessible and fractional accessible and free volumes by eqs. (2), (3), and (5).

The annealed film (sample 2) loses 4.6% of its free volume. Swelling in sc-CO_2 of sample 1 with residual solvent results in an increase of free volume of 6.6%, whereas the free volume increases by 9.9% (Table I) in the annealed film (sample 2).

In order to estimate changes of microstructure and microcavity distribution in the polymeric samples, the samples were examined by atomic force microscopy (AFM) and transmission electron microscopy (TEM); the obtained data are summarized in Table II.

According to AFM, sample 1 consists of particles having a diameter of 25–110 nm [Figure S1(a–c)]. The film contains a small number of microcavities with a broad size distribution. After treatment in sc-CO_2, the number of microcavities increased [Figure S1(d–f)]; their average diameter and its standard deviation decreased.

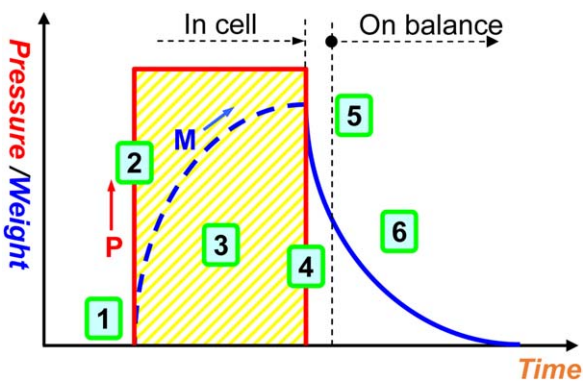

Figure 5. Experimental procedure for sc-CO_2 treatment: (1) sample loading, (2) pressurizing, (3) CO_2 sorption, (4) depressurizing, (5) sample transfer to balance, (6) CO_2 desorption. [Color figure can be viewed in the online issue, which is available at wileyonlinelibrary.com.]

Table I. Changes of Density and Free Volume of the Samples before and after Swelling in sc-CO_2

Sample	Sample 1, before	Sample 1, after	Sample 2, before	Sample 2, after
Density, ρ (g/cm^3)	2.006	1.935	2.000	1.950
Free volume, V_f (cm^3/g)	0.276	0.294	0.263	0.289
ΔV_f		0.018, 6.6%	−0.013, −4.6%	0.026, 9.9%

Table II. Mean-Squared Roughness, Mean Diameter, and Depth of Pores on Surface of Sample 1 before and after Swelling in sc-CO_2 and Sample 2 before Swelling in sc-CO_2

Sample/of the film	Sample 1, before, side 1	Sample 1, before, side 2	Sample 1, after, side 1	Sample 1, after, side 2	Sample 2, before, side 1	Sample 2, before, side 2
R_q[a] (nm)	2–4	21–40	2–9	23–48	5–25	17–22
D[b] (nm)	130	1250	170	380	230	290
ΔD[c] (nm)	80	1230	150	490	150	200
H[d] (nm)	6	83	10	42	9	36
ΔH[e] (nm)	10	87	19	67	9	73

[a] Measured by square frames with 10 μm sides.
[b] Mean diameter of pore.
[c] Standard deviation of pore diameter.
[d] Mean depth of pore.
[e] Standard deviation of pore depth.

The annealing results in particle conglomeration and the nucleation of additional microcavities [Figure S1(g–i)]. The cavity size distribution significantly narrowed, indicating a major rearrangement of the film microstructure. Moreover, film 2 is doubled in thickness, due to the relaxation of mechanical tensions appearing on the interface between the forming polymeric film and the support.

Gas Permeation

The permeability coefficients of gases for sample 1 after swelling in sc-CO_2 become higher by a factor of 2.5 for He, 3.3 for H_2, 3.7 for O_2, 4.0 for N_2, 3.4 for CO_2, and 3.6 for methane (Table III). But the degree of permeability increase is approximately the same for different volumes of gas molecules. That means that the free volume increase due to swelling of sample 1 does not affect the free volume element (microcavity) distribution.

The permeability coefficients of gases for sample 2 before swelling are lower than those for sample 1 before swelling by a factor of 1.1 for He, 1.5 for H_2, 2.8 for O_2, 4.0 for N_2, 3.5 for CO_2, and 7.4 for methane (Table III). So, the higher volume of the gas molecule results in a larger decrease of the gas permeability coefficient. This can be explained by the fact that the annealing of PHFP above the glass-transition temperature leads not only to a complete desorption of residual solvent and a decrease of free volume but also to a size redistribution of the microcavities.

The permeability coefficients of gases in sample 2 obtained after swelling in sc-CO_2 were slightly lower than the corresponding values for sample 1. But, the permeability coefficients in sample 2 before and after the swelling in sc-CO_2 differ by a factor of 2.4 for He, 3.6 for H_2, 5.9 for O_2, 8.1 for N_2, 6.7 for CO_2, and 10.6 for methane (Table III). Besides, the higher volume of the gas molecule results in a larger decrease of the gas permeability coefficient. This means that the free volume increase due to the swelling of sample 2 versus sample 1 leads to a size redistribution of the microcavities.

Table III. Gas Transport Parameters before and after Swelling in sc-CO_2

Sample	V_w of gas molecule (Å^3)	Sample 1, before	Sample 1, after	Sample 2, before	Sample 2, after
Gas	P (Barrer)	P (Barrer)	P (Barrer)	P (Barrer)	
He	—[a]	632	1590	588	1400
H_2	9.78	294	972	201	728
O_2	17.08	79.2	291	27.8	165
N_2	24.38	23.6	95	5.85	47.2
CO_2	30.91	219	750	63.1	421
CH_4	29.64	7.9	28.3	1.07	11.3

[a] The radius of He was not experimentally determined.

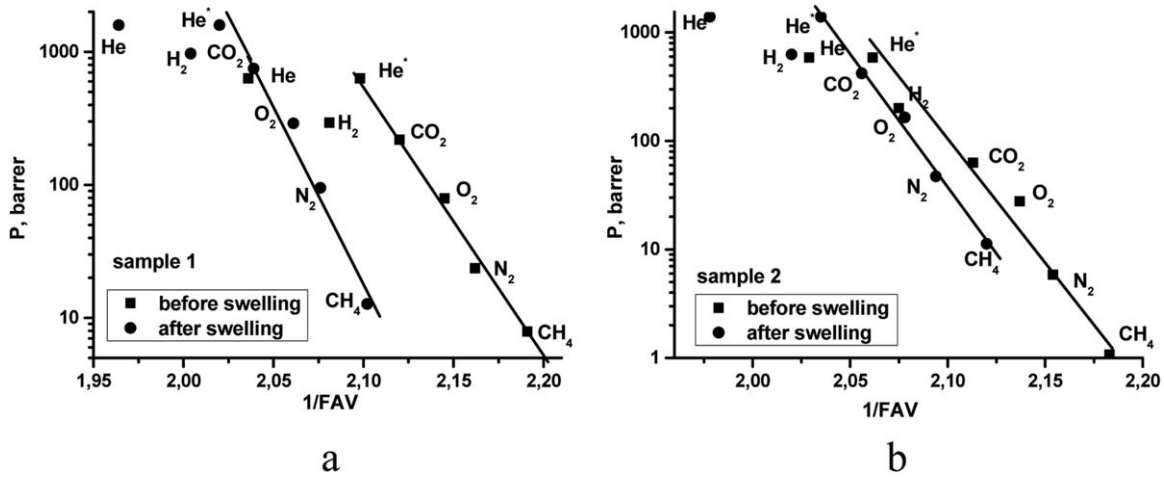

Figure 6. Dependence of permeability coefficients P on the fractional accessible volume (FAV) for sample 1 (a) and sample 2 (b).

Table IV. Parameters of the Line $y = A - Bx$ for Dependence of Permeation Coefficients versus Specific Accessible Volume (1/FAV)

Sample Swelling in sc-CO_2	Sample 1		Sample 2	
	Before	After	Before	After
A	46.61	61.11	46.47	54.40
B[a]	20.88	28.51 (36.5%)	21.20	25.16 (18.7%)
R (%)	99.32	99.06	97.58	99.50

[a] Increase in the B parameter is shown in brackets.

It must be noted that the coefficients of gas permeability in the samples before treatment were 1.5 to 2 times or more lower than in the perfluorinated copolymer AF1600, as previously studied[34] (Table III). However, swelling in the sc-CO_2 environments results in a significant increase in the permeability coefficients in such a way that the permeability coefficients for nitrogen, oxygen, and carbon dioxide are comparable, while for hydrogen and helium the permeability coefficients are superior to the permeability coefficients of AF1600 by 1.5 times. Such a comparison shows that the treatment in the sc-CO_2 environments is an effective instructive technique that can significantly change the gas transport parameters of polymeric membranes.

The dependencies of permeability coefficients before and after CO_2 treatment on fractional accessible volume are demonstrated in Figure 6. All dependencies are linear with a rather high correlation factor ($R > 98\%$) if one excludes helium and hydrogen from the sets of gases. The points for He and H_2 fall out from the overall linear dependencies that were previously observed for He.[18]

Table IV contains the parameters of the dependencies of permeability coefficients on the fractional accessible volume. The B value is a slope of the dependence and corresponds to a total selectivity of a polymer. According to Table IV, the total selectivity of permeability in sample 1 after CO_2 treatment rises by 36%, whereas in annealed sample 2 after the treatment it grows by only 18%, which is almost two times less.

Relaxation Processes

The gas permeability coefficients of sample 1 were measured 3 and 6 weeks after sc-CO_2 treatment (Table V) to monitor the relaxation (aging) process. An evident reduction of permeability coefficients was observed in the 3 weeks of aging (Table V). The permeability coefficients decrease by a factor of 1.3 for He, 1.5

Table V. Change of Permeability Coefficients in Time after CO_2 Treatment

Sample	Sample 1				Sample 2		
Data	12.03	7.04	31.04	$P(1)/P(2)$, $P(2)/(3)$	10.04	4.05	$P(4)/P(5)$
Gas	$P(1)$, Barrer	$P(2)$, Barrer	$P(3)$, Barrer		$P(4)$, Barrer	$P(5)$, Barrer	
He	1590 (632)	1250	1260	1.27, 0.99	1400 (588)	1225	1.14
H_2	972 (294)	684	659	1.42, 1.04	728 (201)	590	1.23
O_2	291 (79.6)	157	143	1.85, 1.10	165 (27.8)	117	1.41
N_2	95 (23.6)	45.9	40.5	2.07, 1.13	47.2 (5.85)	32.6	1.45
CO_2	750 (219)	417	376	1.80, 1.11	421 (63.1)	294	1.43
CH_4	28.3 (7.9)	12.7	10.6	2.23, 1.20	11.3 (1.07)	6.6	1.71

The data before CO_2 treatment are presented in brackets, P(1) was measured at 12.03.2015, P(2) at 7.04, P(3) at 31.04, P(4) was measured at 10.04 and P(5) at 4.05.

Table VI. Comparison of Relaxation after CO_2 Treatment for Two Types of Samples

Sample Gas	Sample 1			Sample 2
	P(1)/*P*(2)	*P*(1)/*P*(3)	Δ	*P*(A)/*P*(B)
He	1.27	1.26	0	1.14
H_2	1.42	1.47	0.05	1.23
O_2	1.85	2.03	0.18	1.41
N_2	2.07	2.34	0.27	1.45
CO_2	1.80	1.99	0.19	1.43

for H_2, 2 for O_2, 2.3 for N_2, 2 for CO_2, and 2.7 for methane. Further aging (for 6 weeks) of sample 1 leads to an insignificant reduction of the permeability coefficients. Thus, we can conclude that the relaxation of PHFP films after swelling in sc-CO_2 is faster than that of swollen poly(ether imide) films.[18]

The relaxation rate of the annealed sample 2 after sc-CO_2 treatment is much lower than the aging rate of sample 1 over the same 3 weeks. (Table V). Hence, one observes an opposite behavior: the larger the size of the penetrant molecule, the greater the loss in permeability coefficient becomes. Table VI combines the data for a comparison of the losses in permeability coefficients through relaxation. The relaxation for sample 1 proceeds more intensively, nevertheless keeping the last values for the aged sample larger than the permeability coefficients of gases in annealed sample 2. Thus, the permeability loss increases with increasing volume of gas molecules. This means that during the aging of the polymeric films a partial contraction of large microcavities takes place.

CONCLUSIONS

We have shown that the gas permeability coefficients for annealed samples after swelling in sc-CO_2 became higher by a factor of 2.4 for He, 3.6 for H_2, 5.9 for O_2, 8.1 for N_2, 6.7 for CO_2, and 10.9 for methane. At the same time, after the relaxation of the samples over 50 days, the permeability coefficients were decreased because of the collapse of certain microcavities. Nevertheless, these coefficients exceeded the original values for the annealed sample for He by 2.0 times, for H_2 2.4, for O_2 1.8, for N_2 1.7, for CO_2 1.7, and for methane 1.3. The permselectivity of the same sample in comparison with the initial one increased by 1.2 times.

Thus, this study shows the effectiveness of both preannealing and subsequent swelling of polymer films in supercritical CO_2 in the improvement of gas transport parameters of the initial film based on a perfluorinated polymer with residual solvent.

The investigation also shows that the modification of polymer films by swelling in sc-CO_2 is an effective method for obtaining selective membranes in the industry.

ACKNOWLEDGMENTS

The work was supported by the Russian Foundation for Basic Research (grant no. 13-08-00520a).

REFERENCES

1. Pixton, M. R.; Paul, D. R. In Polymeric Gas Separation Membranes; Paul D. R., Yampolskii Y. P., Eds.; Boca Raton: CRC Press, **1994**; p 83.
2. Matteucci, S.; Yampolskii, Yu.; Freeman, B. D.; Pinnau, I. In Materials Science of Membranes for Gas and Vapor Separation; Yampolskii, Y., Pinnau, I., Freeman, B. D., Eds.; John Wiley & Sons, **2005**; p. 1.
3. Yampolskii, Y. P. *Russ. Chem. Rev.* **2007**, *76*, 59.
4. Robeson, L. M. *J. Membr. Sci.* **1991**, *62*, 165.
5. Robeson, L. M. *J. Membr. Sci.* **2008**, *320*, 390.
6. Struik, L. C. E. Physical Aging in Amorphous Polymers and Other Materials; Elsevier: New York, **1978**.
7. Pfromm, P. H. In Materials Science of Membranes for Gas and Vapor Separation; Yampolskii Y., Pinnau I., Freeman B. D., Eds.; John Wiley & Sons, **2005**; p 293.
8. Consolati, G.; Genco, I.; Pegoraro, M.; Zanderighi, L. *J. Polym. Sci. Polym. Phys.* **1996**, *34*, 357.
9. Shishatskii, S. M.; Yampolskii, Yu. P.; Peinemann, K. V. *J. Membr. Sci.* **1996**, *112*, 275.
10. McCaig, M. S.; Paul, D. R. *Polymer* **2000**, *41*, 629.
11. Yampolskii, Yu.; Alentiev, A.; Bondarenko, G.; Kostina, Yu.; Heuchel, M. *Ind. Eng. Chem. Res.* **2010**, *49*, 12031.
12. Rezac, M. E.; Le Roux, J. D.; Chen, H.; Paul, D. R.; Koros, W. J. *J. Membr. Sci.* **1994**, *90*, 213.
13. Hong, X.; Yean, Y. C.; Yang, H.; Jordan, S. S.; Koros, W. *J. Macromolecules* **1996**, *29*, 7859.
14. Dlubek, G.; Pionteck, J.; Yu, Y.; Thrunert, S.; Elsayed, M.; Badawi, E.; Krause-Rehberg, R. *Macromol. Chem. Phys.* **2008**, *209*, 1920.
15. Oka, T.; Ito, K.; He, Ch.; Dutriez, C.; Yokoyama, H.; Kobayashi, Y. *J. Phys. Chem. B* **2008**, *112*, 12191.
16. Li, Z. H.; Cheng, C.; Zhan, X. Y.; Wu, Y. P.; Zhou, X. D. *Electrochim. Acta* **2009**, *54*, 4403.
17. Mulder, M. Basic Principles of Membrane Technology; Springer: Netherlands, **1996**.
18. Ronova, I. A.; Alentiev, A. Yu.; Chisca, S.; Sava, I.; Bruma, M.; Nikolaev, A. Yu.; Belov, N. A.; Buzin, M. I. *Struct. Chem.* **2014**, *25*, 301.
19. Belov, N. A.; Zharov, A. A.; Shashkin, A. V.; Shaikh, M. Q.; Raetzke, K.; Yampolskii, Y. P. *J. Membr. Sci.* **2011**, *383*, 70.
20. Ronova, I. A.; Rozhkov, E. M.; Alentiev, A. Yu.; Yampolskii, Yu. P. *Macromol. Theory Simul.* **2003**, 6 (*12*), 425.
21. Rozhkov, E. M.; Schukin, B. V.; Ronova, I. A. *Cent. Eur. J. Chem. (Cent. Eur. Sci. J.)* **2003**, *1*, 402.
22. Plate, N. A.; Yampolskii, Yu. P. In Polymeric Gas Separation Membranes; Paul D. R., Yampolskii Y. P., Eds.; Boca Raton: CRC Press, **1994**; p 155.
23. Ronova, I. A.; Bruma, M. *Struct. Chem.* **2012**, *23*, 47.
24. Dewar, M. J. S.; Zoebisch, Z. F.; Healy, E. F.; Stewart, J. J. *J. Am. Chem. Soc.* **1985**, *107*, 902.

25. Askadskii, A. A. Computational Materials Science of Polymers; Cambridge International Science Publishing: Cambridge, **2003**.
26. Zharov, A. A.; Guzyaeva, I. A. *Russ. Chem. Bull. Int. Ed.* **2010**, *59*, 1225.
27. Yushkin, A.; Grekhov, A.; Matson, S.; Bermeshev, M.; Khotimsky, V.; Finkelstein, E.; Budd, P. M.; Volkov, V.; Vlugt, T. J. H.; Volkov, A. *React. Funct. Polym.* **2015**, *86*, 269.
28. Ronova, I. A.; Nikitin, L. N.; Sokolova, E. A.; Bacosca, I.; Sava, I.; Bruma, M. *J. Macromol. Sci. A* **2009**, *46*, 929.
29. Beckman, E. J. *J. Supercrit. Fluids* **2004**, *28*, 121.
30. Nikitin, L. N.; Nikolaev, A. Y.; Said-Galiyev, E. E.; Gamzazade, A. I.; Khokhlov, A. R. *Supercrit. Fluids Theory Pract.* **2006**, *1*, 77.
31. Nikitin, L. N.; Gallyamov, M. O.; Vinokur, R. A.; Nikolaev, A. Y.; Said-Galiyev, E. E.; Khokhlov, A. R.; Jespersen, H. T.; Schaumburg, K. *J. Supercrit. Fluids* **2003**, *26*, 263.
32. Yampol'skii, Y. P.; Novitskii, E. G.; Durgar'yan, S. G. *Zavod. Lab.* **1980**, *46*, 256.
33. Fielding, R. *Polymer* **1980**, *21*, 140.
34. Alentiev, A. Yu.; Yampolskii, Yu. P.; Shantarovich, V. P.; Nemser, S. M.; Platé, N. A. *J. Membr. Sci.* **1997**, *126*, 123.